Thermal Cycling Effects on the Thermoelectric Properties of *n*-Type In,Ce-Based Skutterudite Compounds

KRISHNENDU BISWAS,[1] M.A. SUBRAMANIAN,[1] MORRIS S. GOOD,[2] KAMANDI C. ROBERTS,[2] and TERRY J. HENDRICKS[3,4]

1.—Department of Chemistry, Oregon State University, Corvallis, OR, USA. 2.—Pacific Northwest National Laboratory, 902 Battelle Boulevard, Richland, WA, USA. 3.—Pacific Northwest National Laboratory-MicroProducts Breakthrough Institute, Corvallis, OR, USA. 4.—e-mail: terry.hendricks@pnl.gov

n-Type In-filled $CoSb_3$ is a known skutterudite compound that has shown promising thermoelectric (TE) properties resulting in high dimensionless figure of merit values at elevated temperatures. Use in various waste heat recovery applications will require survival and operation after exposure to harsh thermal cycling environments. This research focused on uncovering the thermal cycling effects on TE properties of *n*-type $In_{0.2}Co_4Sb_{12}$ and $In_{0.2}Ce_{0.15}Co_4Sb_{12}$ skutterudite compositions as well as quantifying their temperature-dependent structural properties (elastic modulus, shear modulus, and Poisson's ratio). It was observed that the Seebeck coefficient and resistivity increased only slightly in the double-filled In,Ce skutterudite materials upon thermal cycling. In the In-filled skutterudites the Seebeck coefficient remained approximately the same on thermal cycling, while the electrical resistivity increased significantly after thermal cycling. Results also show that the thermal conductivity marginally decreases in the case of In-filled skutterudites, whereas the reduction is more pronounced in In,Ce-based skutterudite compounds. The possible reason for this kind of reduction can be attributed to grain pinning effects due to formation of nanoinclusions. High-temperature structural property measurements (i.e., Young's modulus and shear modulus) are also reported. The results show that these structural properties decrease slowly as temperature increases and that the compounds are structurally stable after numerous (up to 200) thermal cycles.

Key words: In,Ce-based skutterudites, thermoelectric, thermal cycling, structural properties

INTRODUCTION

The efficiency of a thermoelectric (TE) material is determined by its dimensionless figure of merit *ZT*,

which depends on the electronic and thermal properties of the compound as defined by the following equation:

$$ZT = \frac{S^2 \sigma}{\lambda_e + \lambda_L} T, \qquad (1)$$

where S is the Seebeck coefficient, σ is the electrical conductivity, λ_e is the electronic thermal conductivity, λ_L is the lattice thermal conductivity, and T is absolute temperature. Researchers have reported advanced TE materials demonstrating ZT values of 1.6 to 2.4, with at least some of these data occurring at temperatures of 673 K to 973 K.[1–14] Skutterudites belong to the Im-3 space group, having a cubic

R^{2+}: Ba, Sr, Ca, Ag, Pd,

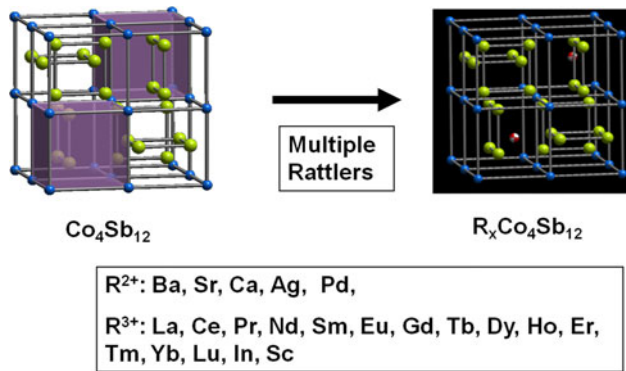R^{3+}: La, Ce, Pr, Nd, Sm, Eu, Gd, Tb, Dy, Ho, Er, Tm, Yb, Lu, In, Sc

Fig. 1. Crystal structure of skutterudite compound with various filler atoms in the void site.

crystal structure as shown in Fig. 1. The structure consists of two voids which are large enough to accommodate various elements of comparable radius to the voids. Elements that can be inserted into the voids are given in the list provided in Fig. 1. The elements inserted into the crystal voids interact and resonate with particular wavelengths of the thermal phonon spectrum, thereby causing them to resonate or "rattle" at that particular wavelength and, ultimately, scatter the thermal phonon rather than allowing it to transmit through the crystal. This effect is responsible for the dramatic reduction of thermal conductivity in filled skutterudites when compared with the unfilled compounds. The more elements that can be filled inside the crystal voids, the more wavelengths or range of wavelengths that can be impacted and scattered, further reducing the lattice thermal conductivity. In addition to the rattling effect, the filler atoms act as a donor impurity, thereby enhancing the electronic properties. This ultimately increases the ZT given by Eq. 1 of skutterudite materials, which already have predominantly high power factors. In 2006, He et al.[15] reported TE properties of $In_xCo_4Sb_{12}$ with ZT values of 1 at 600 K. Subsequently, Subramanian et al. discovered even higher ZT values (1.2 at 600 K) in double-filled skutterudite compositions containing In and a rare earth including Ce.[16] Recent work by Li et al.[17] has shown ZT values of 1.43 at 800 K for $In_{0.2}Ce_{0.15}Co_4Sb_{12}$ fabricated using melt–quench–anneal–spark plasma sintering methods; however, no structural properties were presented in that work. Biswas et al.[18] also showed ZT values of 1.2 to 1.4 at 620 K for n-type $In_{0.2}Ce_yCo_4Sb_{12}$ skutterudite compounds where y = 0.1 to 0.17. The present work is mainly focused on investigating and developing n-type filled skutterudites, the fillers being mainly In and a rare-earth atom such as Ce. The compositions studied in this work were $In_{0.2}Co_4Sb_{12}$ and $In_{0.2}Ce_{0.15}Co_4Sb_{12}$. It is recognized that TE properties (Seebeck coefficient, electrical resistivity, and thermal conductivity) and structural properties [Young's modulus, Poisson's ratio, and coefficient of

thermal expansion (CTE)] are critical to transitioning these promising materials into operating TE devices. Consequently, this work simultaneously characterized both the TE and structural properties for these In,Ce-based skutterudite materials. In addition to the new structural property data on these materials, this work also characterized the thermal cycling behavior of these materials in the temperature range from 300 K to 625 K for the first time.

EXPERIMENTAL PROCEDURES

All the compositions were synthesized by the conventional solid-state reaction method. In, Co, and Sb were mixed together in stoichiometric ratio in a mortar and ground in air. The In-Co-Sb mixture was reacted in a 5% H_2/N_2 gas environment. The sample was heated slowly and calcined in a furnace at temperatures up to 675°C for ~40 h. Thus formed In-Co-Sb sample was combined with Ce that was weighed, mixed, and ground to form the proper stoichiometry in an Ar-filled glove box. The In-Ce-Co-Sb sample was reacted in a 5% H_2/N_2 environment at up to 675°C for 24 h using predetermined heating and cooling ramp rates. The resulting sample was ground again, ball milled, and sintered in a furnace at 675°C. The phase formation was followed at each step by powder x-ray diffraction (XRD) taken on Rigaku Miniflex-II by using Cu K_α radiation with a graphite monochromator. The Seebeck coefficient and electrical resistivity measurements were carried out on ZEM-3 (within an error limit of 5%), and the thermal diffusivity measurements (within an error limit of 10%) were carried out on a Netzsch micro flash instrument. Specific heat measurements were performed using a Mettler differential scanning calorimeter.

This work also investigated and measured the temperature-dependent shear modulus, G, Young's modulus, E, and Poisson's ratio, v, of the $In_{0.2}Co_4Sb_{12}$ and $In_{0.2}Ce_{0.15}Co_4Sb_{12}$ skutterudite materials up to 300°C. These measurements were performed using techniques described by Migliori and Sarrao[19] in a specially designed high-temperature resonant ultrasound (RUS) system shown in Fig. 2. This system was specially designed to perform the RUS measurement technique at temperatures up to 400°C. This system and its sensing transducers were checked and calibrated by measuring a known fused quartz sample at temperatures up to 90°C. The measured Young's modulus (E) and Poisson's ratio (v) of the fused quartz sample (v = 0.156, E = 73.4 GPa) showed good agreement with known literature and manufacturer values (v = 0.17, E = 72.5 GPa). The skutterudite compounds investigated here are isotropic materials because of their basic cubic structure, and therefore their structural properties, E, G, and v, are related by the well-known relationship

Fig. 2. High-temperature RUS chamber capable to 400°C.

$$G = \frac{E}{2(1 + v)}. \tag{2}$$

The RUS technique inputs a vibrational signal to a rectangular parallelepiped sample as shown in Fig. 2 and evaluates the output frequency spectrum from the sample to determine the elastic coefficients, C_{11} and C_{44}, through inverse analysis techniques. These elastic coefficients are then used to determine G, E, and v using

$$G = C_{44}, \tag{3}$$

$$E = \frac{C_{44}(3C_{11} - 4C_{44})}{C_{11} - C_{44}}, \tag{4}$$

$$v = \frac{C_{11} - 2C_{44}}{2(C_{11} - C_{44})}. \tag{5}$$

Equations 3–5 were then used to establish the measurement values that are presented in Fig. 6. The output frequency spectrum and resonances from the sample shifted (and new resonances were created) as temperature increased in the testing. These resonance frequency shifts and new resonances were meticulously tracked to determine the elastic coefficients, C_{11} and C_{44}, as the temperature increased. The uncertainties in the elastic modulus and Poisson's ratio in Fig. 6 were determined to be 4% and 6.5%, respectively.

The CTE up to 400°C determined in this work matched well with values reported in previous work by Biswas et al.[18] These structural properties, G, E, v, and CTE, at high temperatures are important in successfully transitioning these and any TE materials into operating TE devices because they govern the TE material and device component structural stresses that develop in operating devices under temperature differentials experienced in energy recovery applications. The material properties at high temperatures are crucial and necessary inputs to structural finite-element analyses (FEA) that quantify high structural stress levels in TE device designs before fabrication. These properties and FEA analyses are therefore crucial to identifying material and device design parameters and characteristics to minimize the structural stresses and lead to successful TE devices that can survive the inevitable stresses that develop.

RESULTS AND DISCUSSION

Research and development work included investigating thermal cycling effects on the TE properties of several *n*-type In,Ce-based Co_4Sb_{12} materials from 323 K to 673 K (200 cycles) according to the thermal cycling profile shown in Fig. 3. XRD patterns of the compounds given in Fig. 4 indicated single-phase formation, and the peaks were indexed based on the Im-3 space group. The lattice parameters calculated using Le Bail fit agree well with the reported values for the In,Ce-based skutterudite compounds. It is clear from the XRD patterns that the compound is stable and does not degrade after thermal cycling.

Thermal Cycling Effects on the Thermoelectric Properties

The Seebeck coefficients of the $In_{0.2}Co_4Sb_{12}$ and $In_{0.2}Ce_{0.15}Co_4Sb_{12}$ compounds shown in Fig. 5a, e indicate that electrons are the major charge carriers, and the electrical resistivity plots shown in Fig. 5b, f indicate degenerate semiconducting behavior for both compounds. An additional reduction process was carried out after the thermal cycling in the case of In,Ce-based skutterudite compounds to make sure the surface was not oxidized due to the high-temperature thermal environments to which they were subjected. From Fig. 5a, b it is clear that the Seebeck coefficient and electrical resistivity of the $In_{0.2}Ce_{0.15}Co_4Sb_{12}$ compound remained largely the same (slight increase), whereas the thermal conductivity in Fig. 5c shows an enormous decrease after thermal cycling. This ultimately increases the final ZT of the thermally cycled samples from 0.89 to 0.95 as shown in Fig. 5d. Other $In_{0.2}Ce_{0.15}Co_4Sb_{12}$ and
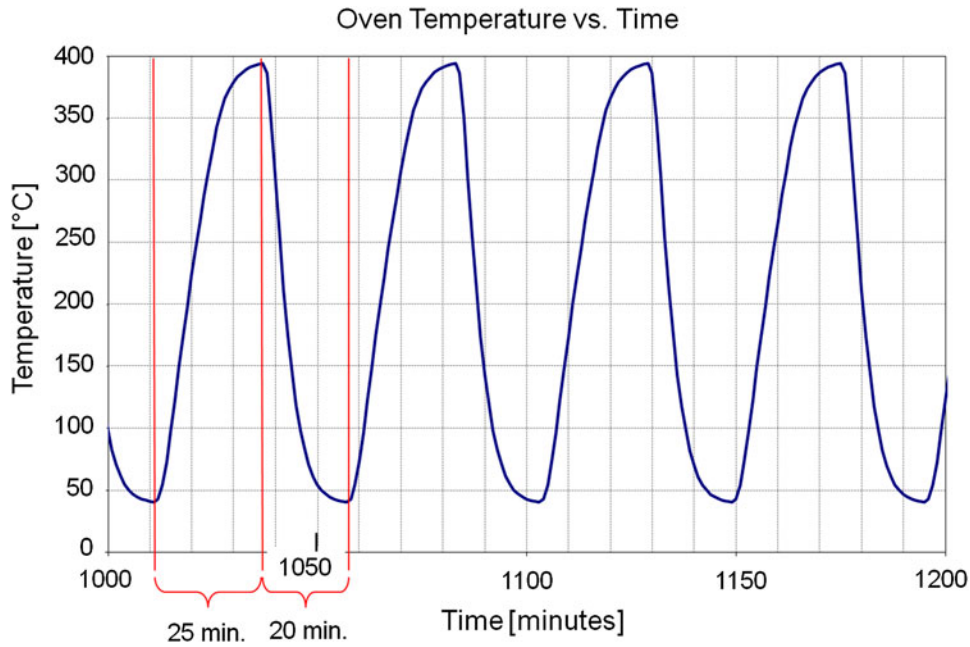
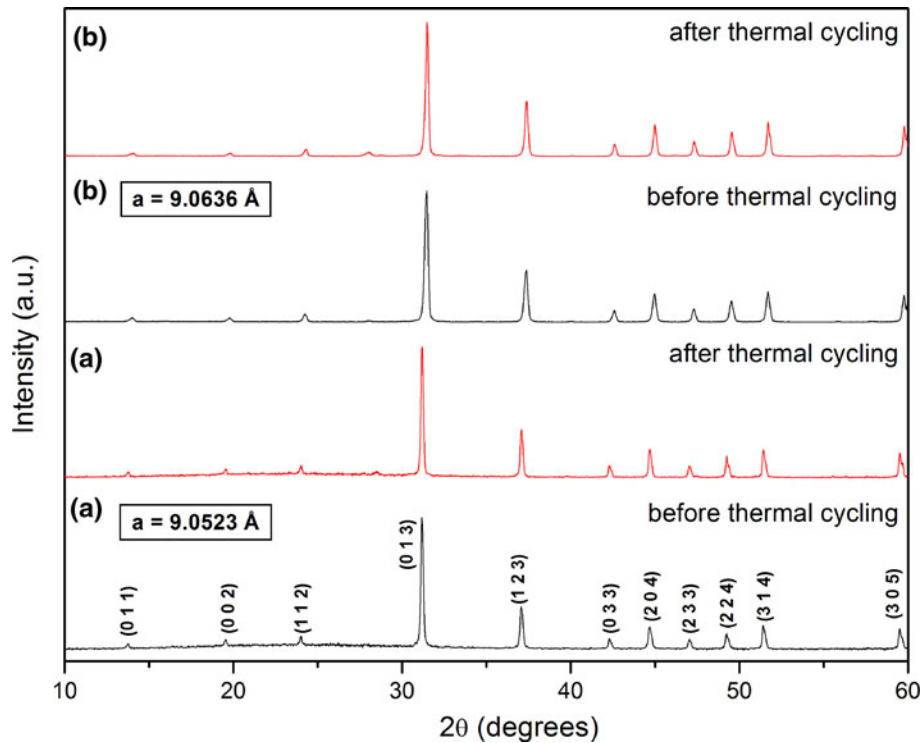Fig. 3. Verified thermal cycling profiles used in the present study.

Fig. 4. XRD patterns of (a) $In_{0.2}Co_4Sb_{12}$ and (b) $In_{0.2}Ce_{0.15}Co_4Sb_{12}$.

$In_{0.2}Ce_{0.1}Co_4Sb_{12}$ samples showed larger increases in Seebeck coefficient and subsequent power factors after thermal cycling, thereby creating a second pathway for ZT enhancement.[18] The Seebeck coefficient and electrical resistivity of the $In_{0.2}Co_4Sb_{12}$

compound shown in Fig. 5e, f show a marginal increase in the Seebeck coefficient but an enormous increase in the electrical resistivity. The thermal conductivity remains almost the same before and after thermal cycling, as is evident from Fig. 5g. The
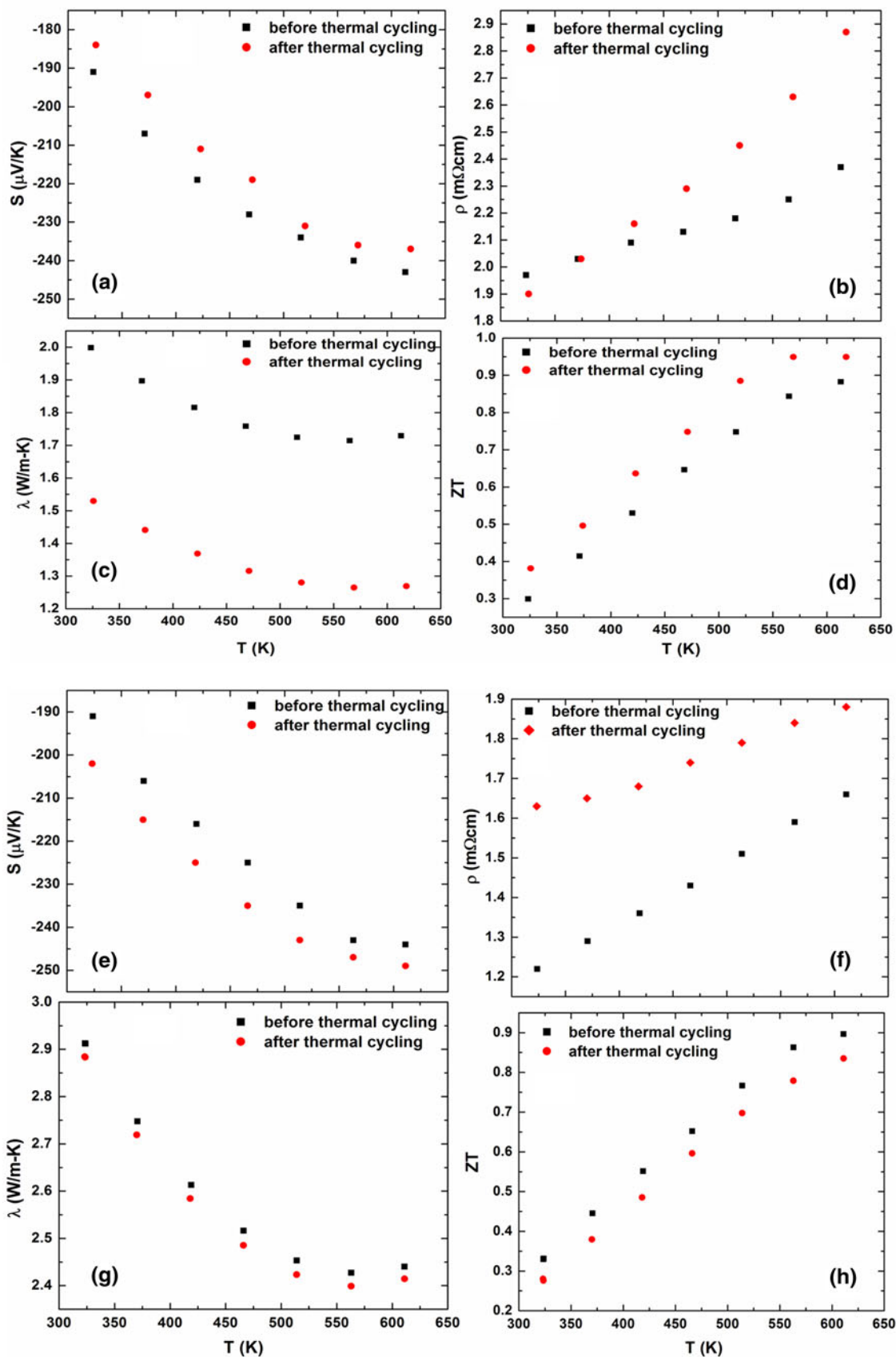
Fig. 5. Thermal cycling effect on TE properties of (a–d) $In_{0.2}Ce_{0.15}Co_4Sb_{12}$ and (e–h) $In_{0.2}Co_4Sb_{12}$.

final result is that the ZT decreases in the $In_{0.2}Co_4Sb_{12}$ compound from ~0.9 to ~0.85 after thermal cycling. Additional samples of $In_{0.2}Co_4Sb_{12}$ also showed only small or no effects on thermal conductivity after thermal cycling.

The increase in ZT of the $In_{0.2}Ce_{0.15}Co_4Sb_{12}$ compound is due to the significant reduction in the thermal conductivity values, which can be attributed to the grain boundary effects known in these compounds. Though the exact reason is not clear now and further experiments are being carried out to explain the behavior, the following hypothesis can be a plausible reason for the observed thermal conductivity reduction: Some of the filler atoms, in this case Ce, being loosely bound, can possibly come out of the crystal structure void site shown in Fig. 1 due to the rapid thermal stresses and form an oxide, such as CeO_2, at the grain boundaries. The CeO_2 thus formed can act as nanoinclusions at the grain boundaries and further scatter the thermal phonons, bringing about a significant reduction in the lattice thermal conductivity. Similar observations were found in $Yb_{0.2}Co_4Sb_{12}/Yb_2O_3$ composite by Zhao et al.,[20] wherein the lattice thermal conductivity reduced while the power factor remained almost the same.

In the case of $In_{0.2}Co_4Sb_{12}$, a similar process can be thought of as occurring, but due to the lesser tendency of indium to form an oxide (lesser affinity for oxygen) when compared with Ce, the formation of an oxide composite is difficult. This ultimately retains the lattice thermal conductivity even after thermal cycling, thereby not affecting the overall thermal conductivity. Since the electrical resistivity (Fig. 5f) increases enormously after thermal cycling, the power factor decreases, thereby ultimately reducing the overall ZT by a small extent.

High-Temperature Structural Properties

Past work with these $In_{0.2}Co_4Sb_{12}$ and $In_{0.2}Ce_{0.15}Co_4Sb_{12}$ skutterudite materials has shown that they are structurally stable during the thermal cycling processes discussed above.[18] Additional high-temperature RUS experimental work was carried out for the first time to measure the structural properties at high temperatures up to 300°C, which adds to the structural property database of these skutterudite materials. Figure 6a, b, and c show the resulting temperature-dependent shear modulus, G, Young's modulus, E, and Poisson's ratio, v, of the $In_{0.2}Co_4Sb_{12}$ and $In_{0.2}Ce_{0.15}Co_4Sb_{12}$ skutterudite samples, respectively.

The shear modulus of the two materials, $In_{0.2}Ce_{0.15}Co_4Sb_{12}$ and $In_{0.2}Co_4Sb_{12}$, generally shows a slow decrease from room temperature to 300°C, with the magnitude of the $In_{0.2}Co_4Sb_{12}$ shear modulus being slightly higher than that of $In_{0.2}Ce_{0.15}Co_4Sb_{12}$ throughout this temperature range. The Young's modulus (i.e., elastic modulus) of the two materials, $In_{0.2}Ce_{0.15}Co_4Sb_{12}$ and $In_{0.2}Co_4Sb_{12}$,
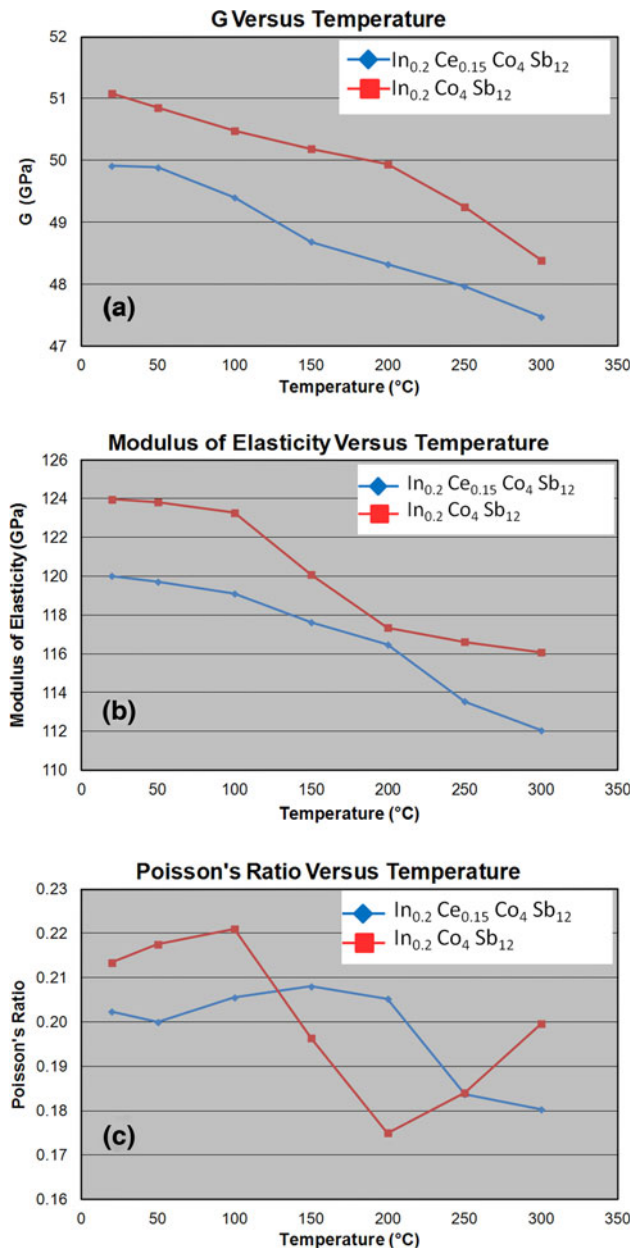

Fig. 6. Temperature-dependent (a) shear modulus, (b) Young's modulus, and (c) Poisson's ratio in $In_{0.2}Ce_{0.15}Co_4Sb_{12}$ and $In_{0.2}Co_4Sb_{12}$ samples up to 300°C (573 K).

generally exhibited a slightly larger percentagewise decrease from room temperature to 300°C than the shear modulus. Additionally, the magnitude of the $In_{0.2}Co_4Sb_{12}$ Young's modulus was slightly higher than that of $In_{0.2}Ce_{0.15}Co_4Sb_{12}$ throughout the temperature range. The Young's moduli for both of these skutterudite materials are slightly lower than the Young's modulus of $Ba_{0.05}Yb_{0.2}Co_4Sb_{12}$ and $Ce_{0.85}Fe_{3.5}Co_{0.5}Sb_{12}$ skutterudite materials (~133 GPa to 136 GPa) and higher than that for lead antimony silver telluride (LAST) and lead antimony silver tin telluride (LASTT) materials (~46 GPa to 55 GPa).[21] These new structural

properties will be crucial in helping to evaluate structural stresses, develop stress-reducing design techniques, and transition these skutterudites into future operating TE devices.

CONCLUSIONS

Thermal cycling effects were carried out in the present study on two skutterudite material systems, viz. $In_{0.2}Co_4Sb_{12}$ and $In_{0.2}Ce_{0.15}Co_4Sb_{12}$. It was found that thermal cycling enhances the *ZT* of the In,Ce-based skutterudite whereas the *ZT* in the $In_{0.2}Co_4Sb_{12}$ compound reduces marginally. The reason for the enhancement of *ZT* in the In,Ce-based skutterudite is predominantly due to the enormous reduction in thermal conductivity after thermal cycling, which in turn can be attributed to grain boundary effects. Due to the high-temperature thermal environments, the In,Ce-based skutterudite can form cerium oxide inclusions at grain boundaries, which helps in effectively scattering thermal phonons within the crystal. Similar oxide formation is not possible in the case of the $In_{0.2}Co_4Sb_{12}$ compound, and hence its thermal conductivity remains nearly the same. Work with other $In_{0.2}Ce_{0.15}Co_4Sb_{12}$ and $In_{0.2}Ce_{0.1}Co_4Sb_{12}$ samples showed larger increases in Seebeck coefficient and subsequent power factors after thermal cycling, thereby creating a second avenue for *ZT* enhancement in these materials. New temperature-dependent structural properties of the $In_{0.2}Co_4Sb_{12}$ and $In_{0.2}Ce_{0.15}Co_4Sb_{12}$ compounds up to 300°C are presented, indicating that the shear and Young's moduli slowly decrease as temperature increases. This new structural property information is just as critical as the TE properties of these In, Ce-based skutterudites in successfully transitioning these materials into future operating TE devices. An actual couple will be built using these *n*-type filled skutterudites and *p*-type lead antimony silver tin telluride (LASTT) compounds to demonstrate a viable commercialization pathway for these materials.

REFERENCES

1. J. Androulakis, K.-F. Hsu, R. Pcionek, H. Kong, C. Uher, J.J. D'Angelo, A. Downey, T. Hogan, and M.G. Kanatzidis, *Adv. Mater.* 18, 1170 (2006).
2. S.R. Brown, S.M. Kauzlarich, F. Gascoin, and G.J. Snyder, *Chem. Mater.* 18, 1873 (2006).
3. T. Caillat, J.-P. Fleurial, and A. Borshchevsky, *J. Phys. Chem. Solids* 58, 119 (1997).
4. E.A. Skrabek and D.S. Trimmer, *Chapter 22 in CRC Handbook of Thermoelectrics*, ed. D.M. Rowe (Boca Raton, FL, USA: CRC, 1995).
5. B.C. Sales, D. Mandrus, B.C. Chakoumakos, V. Keppens, and J.R. Thompson, *Phys. Rev. B* 56, 15081 (1997).
6. Y. Gelbstein, Z. Dashevsky, and M.P. Dariel, *Phys. B* 363, 196 (2005).
7. X. Shi, H. Kong, C.-P. Li, C. Uher, J. Yang, J.R. Salvador, H. Wang, L. Chen, and W. Zhang, *Appl. Phys. Lett.* 92, 182101 (2008).
8. V.K. Zaitsev, M.I. Fedorov, E.A. Gurieva, I.S. Eremin, P.P. Konstantinov, A.Yu. Samunin, and M.V. Vedernikov, *Phys. Rev. B* 74, 045207 (2006).
9. X. Tang, Q. Zhang, L. Chen, T. Goto, and T. Hirai, *J. Appl. Phys.* 97, 093712 (2005).
10. K.-F. Hsu, S. Loo, F. Guo, W. Chen, J.S. Dyck, C. Uher, T. Hogan, E.K. Polychroniadis, and M.G. Kanatzidis, *Science* 303, 818 (2004).
11. J. Androulakis, C.-H. Lin, H.-J. Kong, C. Uher, C.-I. Wu, T. Hogan, B.A. Cook, T. Caillat, K.M. Paraskevopoulos, and M.G. Kanatzidis, *J. Am. Chem. Soc.* 129, 9780 (2007).
12. M. Zhou, J.-F. Li, and T. Kita, *J. Am. Chem. Soc.* 130, 4527 (2008).
13. T.M. Tritt and M.A. Subramanian, *Mater. Res. Soc. Bull.* 31, 188 (2006).
14. R. Venkatasubramanian, E. Siivola, T. Colpitts, and B. O'Quinn, *Nature* 413, 597 (2001).
15. T. He, J. Chen, H.D. Rosenfeld, and M.A. Subramanian, *Chem. Mater.* 18, 759 (2006).
16. M.A. Subramanian, T. He, and J. Krajewski, US Patent 7,723,607 (E.I. du Pont de Nemours and Company, Filed Date: April 14, 2005; Issued: May 25, 2010).
17. H. Li, X. Tang, Q. Zhang, and C. Uher, *Appl. Phys. Lett.* 94, 102114 (2009).
18. K. Biswas, M.G. Good, K.C. Roberts, M.A. Subramanian, and T.J. Hendricks, *J. Mater. Res.* 26, 1827 (2011).
19. A. Migliori and J.L. Sarrao, *Resonant Ultrasound Spectroscopy: Applications to Physics, Material Measurements, and Nondestructive Evaluation* (New York: Wiley, 1997).
20. X.Y. Zhao, X. Shi, L.D. Chen, W.Q. Zhang, S.Q. Bai, Y.Z. Pei, X.Y. Li, and T. Goto, *Appl. Phys. Lett.* 89, 092121 (2006).
21. T.J. Hendricks, T.P. Hogan, E.D. Case, and C.J. Cauchy, "Advanced Soldier Thermoelectric Power System for Power Generation from Battlefield Heat Sources", PNNL Report # PNNL-19342, Prepared Under UNITED STATES DEPARTMENT OF ENERGY Contract DE-AC05-76RL01830, SERDP Project #SI-1652, Final Report to the Strategic Environmental Research and Development Program Office, Arlington, VA, September 2010.